

Mathematical Modeling of Skin Condensers for Domestic Refrigerator

¹Mr. Nitin Ghule, ²Prof.S.D.Mahajan

Department of Mechanical Engineering , Modern college of Engineering , Pune University , Pune ,India

Abstract: A mathematical model of hot-wall condensers used in refrigerators is presented. The model predicts the heat transfer characteristics of condenser and the effects of various design and operating parameters on condenser tube length and capacity. A finite element approach was used to model the condenser. The condenser tube is divided into elemental units, with each element consisting of adhesive tape, refrigerant tube and outer metal sheet. The heat transfer characteristics of each section are then analysed by considering the heat transfer through the tube wall, tape and the outer sheet. Variations in inner heat transfer coefficient and pressure drop are considered depending on temperature, fluid phase, type of flow and orientation of tube. Variation in outer heat transfer coefficient is also taken into account. Various materials were analyzed for the tube, tape and outer sheet.

Keywords: Condenser, Domestic Refrigerator, Heat Transfer.

I. INTRODUCTION

The hot-wall condenser, also known as wrapper type condenser, consists of metal tubing, which is installed by direct contact on the inner surface of the outer plate of side walls of a refrigerator as shown in figure 1. The adhesive foil holds the tube in place and acts as a shield to prevent heat transfer into the refrigerating compartment. Since the condenser tubing is installed in a refrigerator wall, which is usually hot, it is called ‘hot-wall condenser’

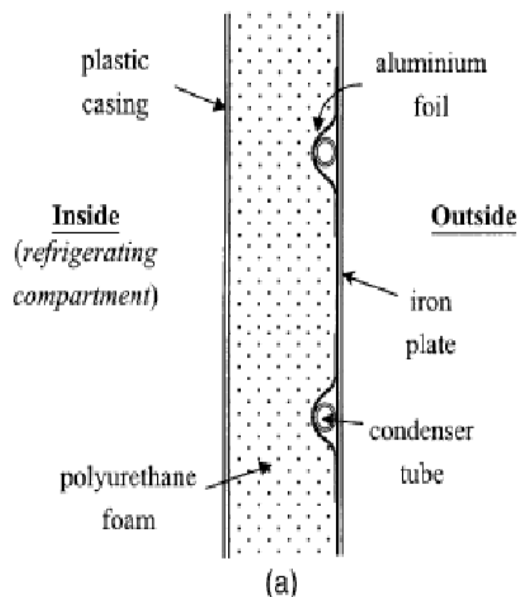


Fig.1. Cross section of a hot-wall condenser on refrigerator wall

1.1 Advantages: Apart from offering better aesthetics and protection from dust, the hot-wall condensers also eliminate the possibility of moisture condensing on the outer surface of the refrigerator.

1.2 Disadvantages: The condenser tube might lose contact with the outer sheet if the aluminum tape loses its adhesion either during foaming or due to alternate heating and cooling during on-and-off cycles. This will affect the heat rejection capacity of the condenser seriously. In addition, compared to external condenser, the heat transfer rate to the refrigerant compartment could be higher due to higher outer wall temperature.

1.3 Mode of Heat Transfer: A significant part of the heat transferred from refrigerant to condensing tube is conducted to the aluminium tape, and a major portion of this flows along the aluminium tape to the outer sheet, from where it is rejected to the ambient. Some amount of heat transfer takes place from the condenser tube to the outer sheet through the air pocket formed between the tube, aluminium sheet and the outer sheet. Direct heat transfer from the refrigerant tube to the outer sheet is expected to be small as there is a line contact between the copper tube and the outer sheet. This heat transfer becomes significant in the case of D-type condenser tube in which this heat transfer has been accounted by an additional term.

1.4 Salient Features:

- This study presents a complete mathematical model of hot-wall condenser that includes the important effect of aluminium tape.
- The model considers the variation in refrigerant and air properties in different regions, variation in inner heat transfer coefficient depending on temperature, phase, and type of flow and orientation of tube and variation in ambient heat transfer coefficient over the outer surface.
- Effect of pressure drop is also taken into account and suitable pressure drop correlations are used depending on the fluid phase.
- Using the model, temperature and pressure variation along the length of the tube can be obtained.
- Similarly temperature variation along the length of the tape and effect of tape angle and length on required tube length can be obtained.
- Different materials for the tube, tape, outer sheet have been considered as well.
- Two different types of tubes namely O type and D type have been modelled.

Hence this model can be used in accurate design and simulation of a hot-wall condenser.

II. MODELLING OF ELEMENTAL CONDENSER

2.1 Modelling Of Elemental Condenser:

In the present analysis, the contribution of the tape is considered by treating it as a fin. It is assumed that the insulation is perfect and there is no heat transfer through the insulation. It is further assumed that all the condensing tubes are identical in construction and each tube with the aluminium tape and outer sheet is symmetrical about the axis A-A'. Hence only one-half of the tube is considered for analysis. As shown in the fig. 2, the complete heat transfer area can be divided into four portions.

Part 1 contains the portion of the tape attached to the tube. The tape is insulated on the other side as shown. The heat transfer in part 1 takes place from refrigerant to condensing tube and then to the tape.

Part 2 contains the tape, which faces the cavity on one side and insulation on the other side. In part 2 heat is carried from section 1-1' to 2-2', with some portion of the heat released to the cavity. The heat released by the tape to the cavity and the heat released to the cavity by the tube facing the cavity is rejected to the ambient air via the outer metal sheet wall.

Part 3 contains tape attached on the metal sheet and

Part 4 contains the metal sheet alone. These portions release the heat coming from section 2-2' to the ambient air.

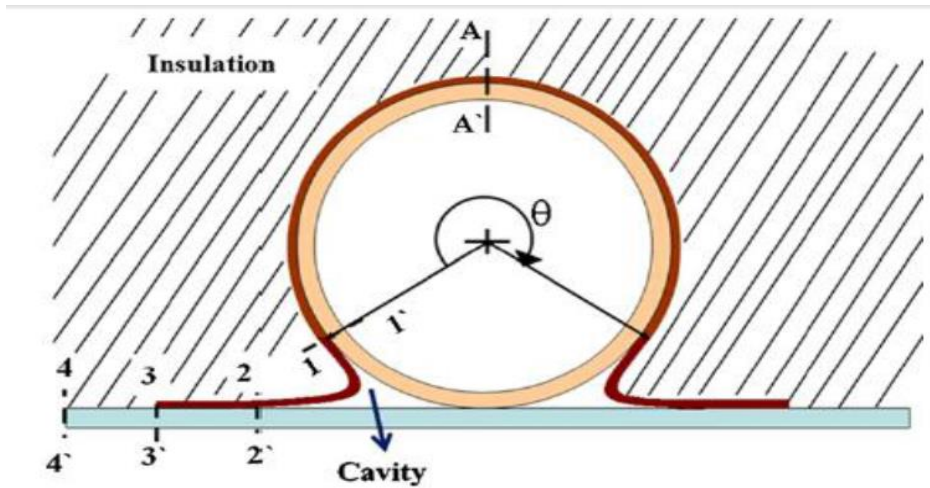


Fig.2. Cross- section view of elemental unit for O type condenser tube

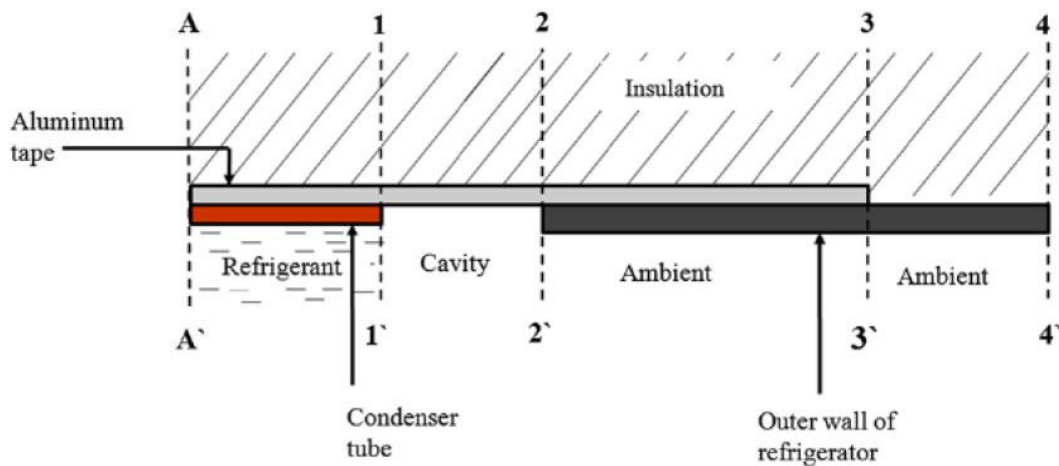


Fig.3. Detailed fin model of one-half of the elemental unit

A steady one-dimensional analysis is carried out for the fin. The cavity and refrigerant temperatures vary along the length of the tube, but are assumed to be constant for a given elemental portion. The cavity temperature (which is not equal to the refrigerant temperature) is calculated by applying energy balance to the cavity. In addition to these the heat transfer coefficients on the cavity and refrigerant sides are assumed to be constant for the elemental portion. The tip (section 4-4') and section A-A' are assumed to be adiabatic. The contact resistance of the tape can be neglected compared with other resistance. Thus the temperature in the region 3-3' can be assumed to be equal for tape and outer sheet.

Now by treating each section separately as a composite fin, the heat transfer model for the element can be developed. The basic governing equation for all the sections can be written in the form of a fin equation as

$$\frac{d^2 \theta_i}{dx^2} - m_i^2 \theta_i = 0 \quad (1)$$

where the values of θ_i and m_i are range of applicability of the equation for different sections are shown in Table 1. The general solution of the differential equation is

$$\theta_i = C_j \exp(m_i X) + C_k \exp(-m_i X) \quad (2)$$

where C_j and C_k are constants which are different for different sections.

TABLE 1- Definitions of θ_i and m_i for different section

Section	θ_i	m_i	Range of applicability
1	$T_{\text{tape}} - T_{\text{rf}}$	$\sqrt{P_{\text{tape}} / (k_{\text{tape}} A_{\text{tape}} ((1/hc_{\text{rf}}) + (t_{\text{ct}}/k_{\text{ct}})))}$	$0 < x < l_1$
2	$T_{\text{tape}} - T_o$	$\sqrt{(P_{\text{tape}} hc_o) / (k_{\text{tape}} A_{\text{tape}})}$	$l_1 < x < l_2$
3	$T_{\text{tape}} - T_a$	$\sqrt{P_{\text{tape}} / (k_{\text{tape}} A_{\text{tape}} ((1/hc_a) + (t_{\text{os}}/k_{\text{os}})))}$	$l_2 < x < l_3$
4	$T_{\text{os}} - T_a$	$\sqrt{(P_{\text{os}} hc_a) / (k_{\text{os}} A_{\text{os}})}$	$l_3 < x < l_4$

There would be eight such constants, values of which can be calculated by using eight boundary conditions. These boundary conditions are obtained by equating temperatures and heat transfer rates at the interfaces 1-1', 2-2' and 3-3' as shown in Fig. 3. This would give six boundary conditions. The remaining two boundary conditions are obtained by assuming the ends A-A' and 4-4' to be adiabatic. The temperature of the cavity which is also a variable, is obtained by balancing heat transfer rates at the cavity as shown in Fig. 4, i.e.,

$$Q_1 + Q_2 = Q_3 \tag{3}$$

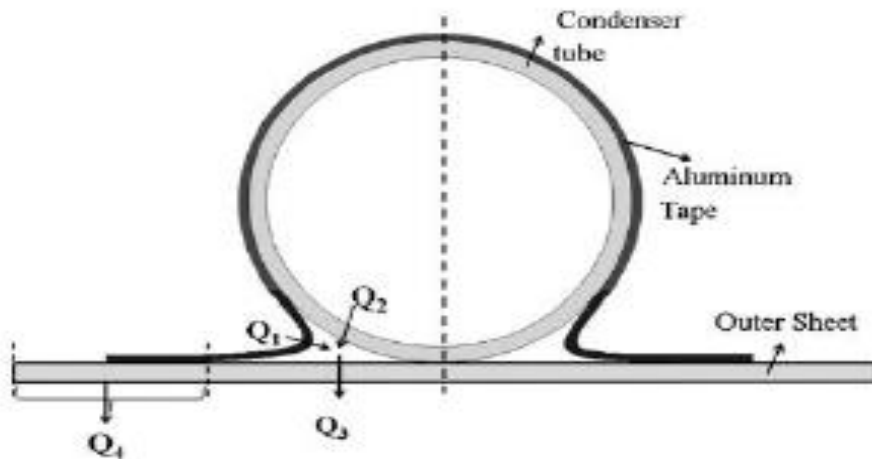


Fig.4. - Heat transfer in the cavity and through outer wall

2.2 Extension of elemental model to whole condenser :

Once the temperature variation in an elemental unit is known, the net heat transfer rate from the element can be calculated as depicted in Fig. 4

Q_{out} = Net heat transfer rate from an element with refrigerant at temperature

$$Q_{out} = 2 * (Q_3 + Q_4) \tag{4}$$

In a refrigerant condenser, the refrigerant generally goes through three different regions namely superheated vapor region, two-phase (vapor-liquid) region and sub-cooled liquid region. Ideally pressure inside the condenser tube remains constant and temperature varies continuously in superheated and sub-cooled region, while in the saturation region temperature remains constant for a pure fluid. But because of friction, gravity and deceleration there is a change in pressure in the direction of refrigerant flow. As a result of the pressure variation there would be a temperature variation in the condensation zone also. As there are different regions, refrigerant properties as well as the correlations for heat transfer coefficient and pressure drop will vary depending on the region. The inner convective heat transfer coefficient depends on refrigerant properties, flow properties, flow regime and orientation of tube, and hence varies along the direction of

refrigerant flow. At the same time the temperature of the outer wall also changes from element to element and so does the ambient heat transfer coefficient. Now considering all these variations and using the appropriate correlations, heat transfer rate from each element can be calculated taking piecewise constant refrigerant temperature. The temperature for the next element in the direction of refrigerant flow for single-phase can be calculated using

$$T_{rf} = T_{rf}^0 - \frac{Q_{out}}{m_{rf} C_{p,rf}} \quad (5)$$

And for two-phase, enthalpy for the next element can be calculated using

$$h_{rf} = h_{rf}^0 - \frac{Q_{out}}{m_{rf}} \quad (6)$$

Now marching in the direction of refrigerant flow by considering small elements till the desired condition for the region is achieved using either of Eqs. (5) or (6). The inlet condition to the condenser is the state of refrigerant at the exit of compressor, obtained from appropriate evaporator conditions and compressor isentropic efficiency. The exit condition of the condenser depends on the required degree of sub-cooling.

2.3 Computation Of Mass Flow Rate:

Mass flow rate of the refrigerant is given by

$$m_{rf} = \frac{\eta_v V_s f}{v_{suc}} \quad (7)$$

Where v_{suc} Specific Volume at suction

f is Frequency of the motor defined as $f = \frac{rpm_{motor}}{60}$

The volumetric efficiency of the compressor with clearance is given by

$$\eta_{v,cl} = \left(1 - \frac{V_c}{V_s} \left[r_p^{1/\gamma} - 1 \right] \right) \quad (8)$$

Where r_p is the Pressure ratio defined as $\frac{P_{dis}}{P_{suc}}$

For a given condensing temperature (or pressure), the pressure ratio r_p increases as the evaporator temperature (or evaporator pressure) decreases. Hence, from the expression for clearance volumetric efficiency, it is obvious that the volumetric efficiency decreases as evaporator temperature decreases.

Effect of Pressure Drops:

This pressure drop can have adverse effect on compressor performance as the suction pressure at the inlet to the compressor P_{suc} will be lower than the evaporator pressure as shown in Fig.5. As a result, the pressure ratio and discharge temperature increases and density of refrigerant decreases. This in turn reduces the volumetric efficiency, refrigerant mass flow rate and increases work of compression. This pressure drop depends on the speed of the compressor and design of the suction valve. The pressure drop increases as piston speed increases. Even though the pressure drop across the discharge valve is not as critical as pressure drop across the suction valve, it still affects the compressor performance.

The net effect of pressure drops across the valves is to reduce the capacity of the system and increase power input. The pressure drop also affects the discharge temperature and compressor cooling in an adverse manner.

Effect of Leakage:

In actual compress refrigerant leakage losses take place between the cylinder walls and the piston, across suction and discharge valves and across the oil seal in open type of compressors. The magnitude of these losses depends upon the

design of the compressor valves, pressure ratio, compressor speed and the life and condition of the compressor. Leakage losses increase as the pressure ratio increases, compressor speed decreases and the life of compressor increases. Due to the leakage, some amount of refrigerant flows out of the suction valves at the beginning of compression stroke and some amount of refrigerant enters the cylinder through the discharge valves at the beginning of suction stroke. The net effect is to reduce the mass flow rate of refrigerant. Even though it is possibly to minimize refrigerant leakage across cylinder walls, eliminating leakages across valves is not possible as it is not possible to close the valves completely during the running of the compressor.

As a result of the above deviations, the actual volumetric efficiency will be lower than the clearance volumetric efficiency. It is difficult to estimate the actual efficiency from theory alone.

$$\eta_{v,cl} = \frac{T_{evap-exit}}{T_{suc}} \left(1 - \frac{V_c}{V_s} \left[r_p^{1/\gamma} - 1 \right] \right) - l^* r_p \quad (9)$$

Where is the leakage loss fraction which is around .015 usually. L

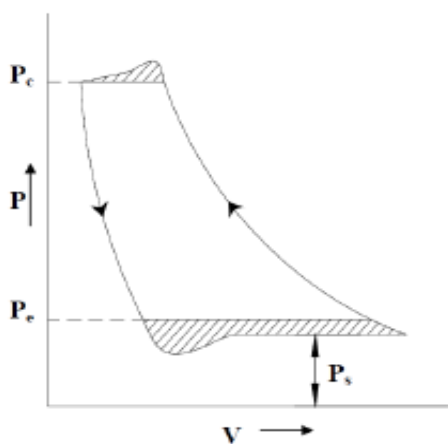


Fig. 5. Effects of suction and discharge side pressure drops on P-V diagram of Compressor.

2.4 Computation of Heat Transfer Coefficients:

2.4.1 Computation of Outer Heat Transfer Coefficient:

The heat transfer from the outer sheet to the ambient is through convection and radiation. And hence the outer heat transfer coefficient is the summation of convection and radiation heat transfer coefficients.

$$hc_a = hc_{a,c} + hc_{a,r} \quad (10)$$

where the average convective heat transfer is calculated from Nusselt number as

$$hc_{a,c} = \frac{\overline{Nu}_a k_{air}}{L_{cha}} \quad (11)$$

where average Nusselt number correlation for vertical flat plate in case of natural convection is given by [2]

$$\overline{Nu}_a = \left(0.825 + \frac{0.387 Ra_a^{1/6}}{\left[1 + \left(\frac{0.492}{Pr_{air}} \right)^{9/16} \right]^{8/27}} \right)^2 \quad (12)$$

Where

$$Pr_{air} = \frac{\mu_{air} C_{p,air}}{K_{air}} \quad (13)$$

$$Ra_a = \frac{g \beta (T_m - T_a) L_{cha}^3}{\nu_{air} \alpha_{air}} \quad (14)$$

and radiative heat transfer coefficient can be calculated using:

$$hc_{a,r} = \frac{\epsilon \sigma (T_m^4 - T_a^4)}{(T_m - T_a)} \quad (15)$$

Where,

$$\sigma = 5.567 \times 10^{-8} \text{ W m}^{-2} \text{ K}^{-4}$$

T_m is the mean surface temperature of the plate portion taken into account and is given by:

$$T_m = T_a + \frac{Q_{out}}{hc_a A_{ele}} \quad (16)$$

All the properties are calculated at temperature (T_m + T_a)/2.

Now h_{ca} is required to calculate mean surface temperature, which in turn is required to calculate the air properties required in the calculation of h_{ca}. Hence an iterative process has to be used to solve the problem. A value of 4-6 W/(m²K) is assumed for h_{ca} initially and Q_{out} is calculated, which is then used to calculate T_m, which is used to get h_{ca}. This procedure is continued until there is very less (~ 0.01) order of difference between old and new h_{ca}.

2.4.2. Computation Of Inner Heat Transfer Coefficient:

2.4.2.1. Single-Phase.

For single-phase flow convective heat transfer coefficient can be calculated depending on whether the flow is laminar or turbulent. For turbulent flow, correlation for Nusselt number is [2]

$$\overline{Nu_{rf}} = 0.23 Re_{rf}^{0.8} Pr_{rf}^{0.3} \quad (17)$$

and for laminar flow, correlation for Nusselt number is [2]

$$\overline{Nu_{rf}} = 3.66(\text{const.walltemp}) \quad (18)$$

Using Nusselt number convective heat transfer coefficient is calculated using:

$$hc_{a,rf} = \frac{\overline{Nu_{rf}} k_{rf}}{d_i} \quad (19)$$

2.4.2.2. Two-Phase Region:

For two-phase region in addition to flow and refrigerant properties, convective heat transfer coefficient depends on type of flow as well as on the orientation of the tube. Hence from the orientation of tube and flow regime inner heat transfer coefficient can be calculated as given below.

For horizontal portion of the tube:

The main criterion used is the ratio of shear to gravity forces. In this paper Breber criterion [5] is adopted to identify different flow regimes. This can be easily determined using Wallis dimensionless gas velocity and Martinelli parameter given by:

$$j_g^* = \frac{x \dot{m}_{rf}}{\pi d_i^2 \sqrt{d_i g \rho_v (\rho_l - \rho_v)}} \quad (20)$$

Wallis dimensionless gas velocity = j_g^*

$$X^2 = \left(\frac{1-x}{x} \right)^{2-n} \left(\frac{\nu_l}{\nu_v} \right)^n \frac{\rho_v}{\rho_l} \quad (21)$$

Lockhart- Martinelli parameter = X^2

For both $j_g > 1.5$; $X_{tt} < 1$ annular flow and $j_g > 1.5$; $X_{tt} > 1.5$ bubble flow, correlation for Nusselt number is given by: [7]

$$Nu_{rf} = 0.05 Re_{rf}^{0.8} Pr_1^{0.33} \tag{22}$$

$$hc_{c,rf} = \frac{Nu_{rf} k_1}{d_i} \tag{23}$$

Where,

$$Re_{rf} = Re_v \left(\frac{\mu_v}{\mu_1} \right)^{2-n} \left(\frac{\rho_1}{\rho_v} \right)^{0.5} + Re_e \tag{24}$$

$$Pr_1 = \frac{\mu_1 C_{p,1}}{k_1} \tag{25}$$

For both $j_g < 1.5$; $X_{tt} > 1.5$ slug flow and $j_g < 0.5$; $X_{tt} < 1.0$ stratified flow correlation for convective heat transfer coefficient is, [10]

$$hc_{c,rf} = \Omega \left[\frac{(\rho_1 (\rho_1 - \rho_v) q h_{fg} k_1^3)}{(d_i \mu_1 \nabla T)} \right]^{0.25} \tag{26}$$

Where,

$$\Omega = 0.728 \alpha_g^{1/4} \tag{27}$$

$$\alpha_g = \frac{1}{1 + [(1-x)/x] (\rho_v/\rho_1)^{2/3}} \tag{28}$$

For vertical tube:

For upward flow, correlation for convective heat transfer coefficient is

$$hc_c = 1.47k \left[\frac{\rho_1 (\rho_1 - \rho_v) g}{\mu^2 Re_1} \right]^{1/3} \tag{29}$$

For downward flow correlation for convective heat transfer coefficient depends on Reynolds number. For $Re \geq 40$ it is given by

$$hc_c = 1.1k \left[\frac{\rho_1 (\rho_1 - \rho_v) g Re_1}{\mu^2} \right]^{1/3} \tag{30}$$

and for higher Reynolds number higher of the two coefficients given below is chosen.

$$hc_c = 0.8k Re_1^{-0.22} \left[\frac{\rho_1 (\rho_1 - \rho_v) g}{\mu^2} \right]^{1/3} \tag{31}$$

$$hc_c = 0.023k Re_1^{1/4} \left[\frac{\rho_1 (\rho_1 - \rho_v) g}{\mu^2} \right]^{1/3} \tag{32}$$

2.5. Computation Of Pressure Drop:

2.5.1. For Single-Phase:

The main cause of drop in pressure in the direction of flow in single-phase region is friction between the fluid and the wall. The correlation for pressure drop is, [6]

$$\left(\frac{dp}{dz}\right)_f = \frac{-8f \cdot \dot{m}_{rf}^2}{\pi^2 \rho_{rf} d_i^5} \quad (33)$$

Where,

$$f = \frac{64}{\text{Re}_{rf}} \text{ , (for laminar flow)} \quad (34)$$

$$f = \left(0.79 \ln \text{Re}_{rf} - 1.64\right)^2 \text{ , (For Turbulent Flow)} \quad (35)$$

2.5.2. For two-phase flow:

In case of two-phase flow because of pressure drop, temperature falls in the direction of flow. This results in a change in the driving temperature drop decisive for heat transfer along the flow path. The total pressure drop in two-phase region is composed of three parts:

Geodetic pressure drop: It is due to gravitational force acting on the fluid. It disappears in horizontal flows. It is given by (Baehr and Stephan, 1998):

$$-\left(\frac{dp}{dz}\right)_{gr,rf} = \alpha \rho_v + (1-\alpha) \rho_l \cdot g \sin(\text{angle}) \quad (36)$$

Here ‘angle’ is the angle of tube with the horizontal,

Frictional pressure drop: The pressure drop due to friction constitutes the major portion of the total pressure drop. It includes not only the momentum transfer between the fluid and the wall but also the momentum transfer between the individual phases [6]. It is evaluated using two different correlations :

a) R.w. Lockhart, R.C. Martinelli correlation

$$-\left(\frac{dp}{dz}\right)_{f,rf} = \phi_1^2 \left(\frac{dp}{dz}\right)_1 \quad (37)$$

$$X_{tt}^2 = \left(\frac{1-x}{x}\right)^{2-n} \left(\frac{v_1}{v_v}\right)^n \frac{\rho_v}{\rho_1} \quad (38)$$

Where n is 0.2

$$\phi_1^2 = 1 + \frac{20}{X_{tt}} + \frac{1}{X_{tt}^2} \quad (39)$$

And

$$-\left(\frac{dp}{dz}\right)_L = \frac{8f \cdot \dot{m}^2 (1-x)^2}{\pi^2 \rho d_i^5} \quad (40)$$

b) Friedel Correlation:

Instead of ϕ_1^2 friedel developed ϕ_{fr}^2 defined as

$$\phi_{fr}^2 = E + \left(\frac{3.24FH}{Fr_H^{0.45} We_L^{0.035}} \right) \quad (41)$$

$$Fr_H = \frac{m_{rf}^2}{gd_i \rho_H^2}$$

$$E = (1-x)^2 + x^2 \frac{\rho_1 f_v}{\rho_v f_1}$$

$$F = x^{0.78} (1-x)^{0.224}$$

$$H = \left(\frac{\rho_1}{\rho_v}\right)^{0.91} \left(\frac{\mu_v}{\mu_1}\right)^{0.19} \left(1 - \frac{\mu_v}{\mu_1}\right)^{0.7}$$

Where,

$$We_1 = \frac{m_{rf}^2 d_i}{\sigma \rho_H} \tag{42}$$

$$\rho_H = \left(\frac{x}{\rho_v} + \frac{1-x}{\rho_1}\right)^{-1} \tag{43}$$

Acceleration pressure drop: It arises because of change in momentum in both phases and is given by [6].

As the outlet density, ρ_o is not known, initially, set $\Delta Pa = 0$ and the outlet elemental pressure, P_{out} is evaluated. Subsequently ρ_o can be found using REFPROP as $q_o \rho_o = \text{function}(P_{out}, E_{ho})$. The whole process is iterated until ρ_o converges.

$$\Delta P_a = (P_o + P_i)_a = G^2 \left[\frac{1}{\rho_o} - \frac{1}{\rho_i} \right] \tag{44}$$

$$\Delta P_{ele} = P_{out,ele} - P_{in,ele} = \Delta P_f + \Delta P_g + \Delta P_a \tag{45}$$

Note that for pressure loss at bend, the frictional component is given by

$$\Delta P_f = K \rho \left(\frac{V^2}{2g} \right) \tag{46}$$

where $K = 0.4$ for the current bend geometry.

The total pressure loss and heat transfer is simply the sum of all elemental pressure losses and heat transfer, which are updated after each iteration:

$$\Delta P_{tot} = \sum \Delta P_{ele} \tag{47}$$

$$\dot{Q}_{tot} = \sum \dot{Q}_{ele} \tag{48}$$

The computation process is repeated for subsequent elements where the inlet conditions of the current element are equal to the outlet conditions of the previous element, namely:

$$\left(T_i \ P_i \ \rho_i \ q_{ref,i} \ E_{hi,i} \right) = \left(T_o \ P_o \ \rho_o \ q_{ref,o} \ E_{ho,i-1} \right) \tag{49}$$

This yields the computation of the condenser capacity, pressure drop and the length.

III. RESULTS

3.1 Modelling Results for 450L model:

Input Parameters:

Refrigerant	R134a
Material of the outer sheet	Mild Steel
Material of the tape	Al
Material of the condenser tube	Mild Steel
Type of tube	O type
Compressor	ADW66AK

Name	Quantity	Unit of measurement
Ambient Temperature	43	°C
Evaporator Exit refrigerant temperature	-25	°C
Suction Temperature	42.33	°C
Discharge Temperature	107.76	°C
Evaporator Exit refrigerant pressure	-3.15	psig
Condenser Inlet refrigerant pressure	190.74	psig
Outer Diameter of Tube	0.0042	m
Thickness of Tube	0.00051	m
Percentage of tube in contact with tape	70	%
Thickness of Outer Sheet	0.0003	m
Thickness of Tape	0.00003	m
Length of single condenser tube	1.207	m
Number of rows	14	
Pitch	0.046	m
Heat Loop Length	6.2	m
Element Length	10	mm

Output Values:

Name	Quantity	Unit of measurement
Mass Flow Rate	0.47848	grams/s
Exit Temperature	52.03756	Celsius
Exit Pressure	201.1238	psi
Exit Enthalpy	304.982	KJ/kg
Exit Quality	0.20243	
Total Pressure Drop	4.132017	psi

3.2 Variations along the condenser and heat loop length:

Using the model presented above, the variation of different parameters along the length of the condenser at mean operating and geometric parameters are obtained. The model captures the variation of temperature and pressure along the tube length very well as shown in Fig. 6. And Fig. 7. It can be seen that in addition to de-superheating and sub-cooling zones there is a continuous drop in temperature in saturation zone too due to pressure drop in the direction of flow. It is observed that the length required for the condensation zone is quite high due to the higher amount of heat transferred during phase change. It is also clear that the pressure drop is higher in two-phase zone due to the additional loss that occurs because of friction between the two phases.

The steps in the pressure graph are due to the heat loop, which has both horizontal and vertical tubes alternating. Since the horizontal tubes have lower pressure drops they appear as horizontal lines on the graph.

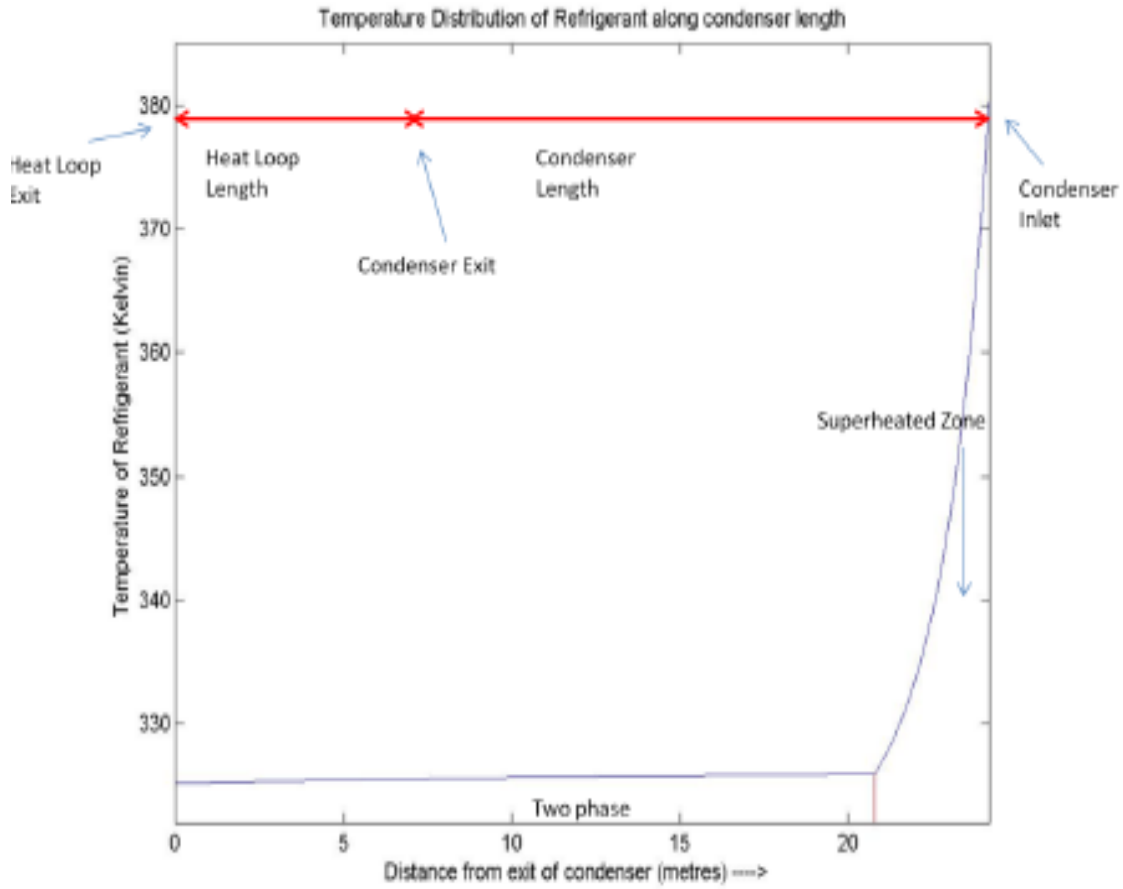


Fig. 6. Temperature Distribution along condenser and Heat loop length

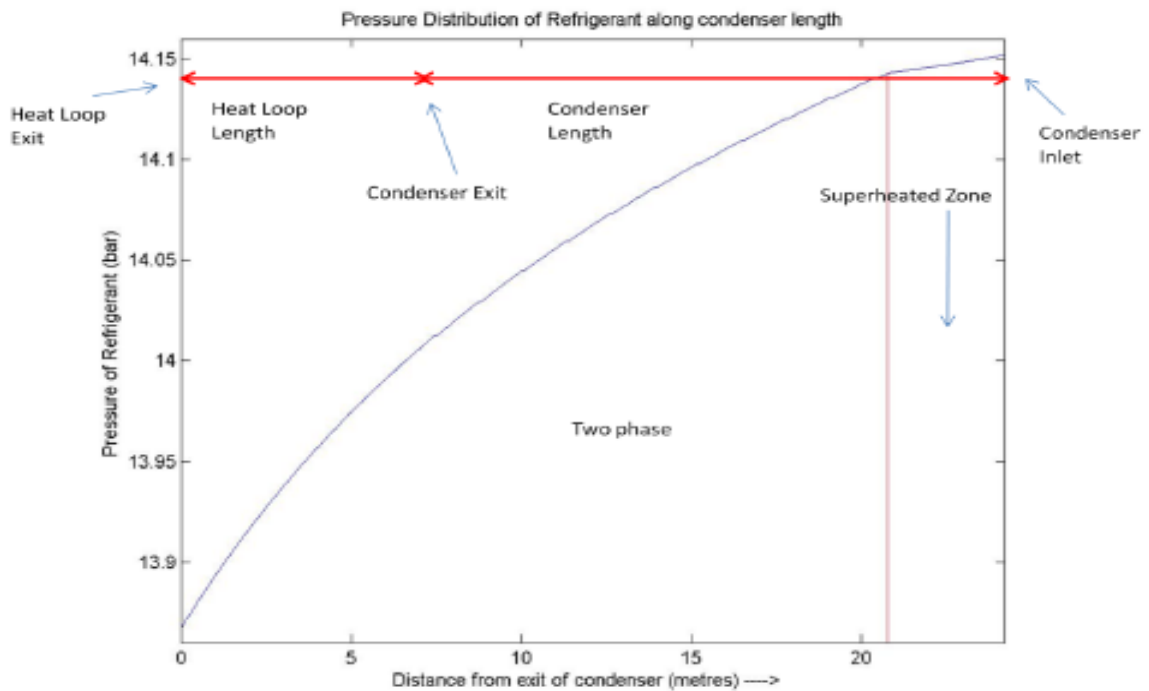


Fig.7. Pressure Distribution along condenser and heat loop length.

3.3 Variations along the tape width:

Fig.8. shows temperature variation along the aluminium tape. It can be seen that the temperature variation is continuous. It can be seen that as the refrigerant moves through the condenser its temperature decreases and thus the tape temperature distribution also decreases. As is obvious the temperature difference between the two consecutive curves in the two phase is very less, and thus all the two phase curves are condensed in a very small area and overlap.

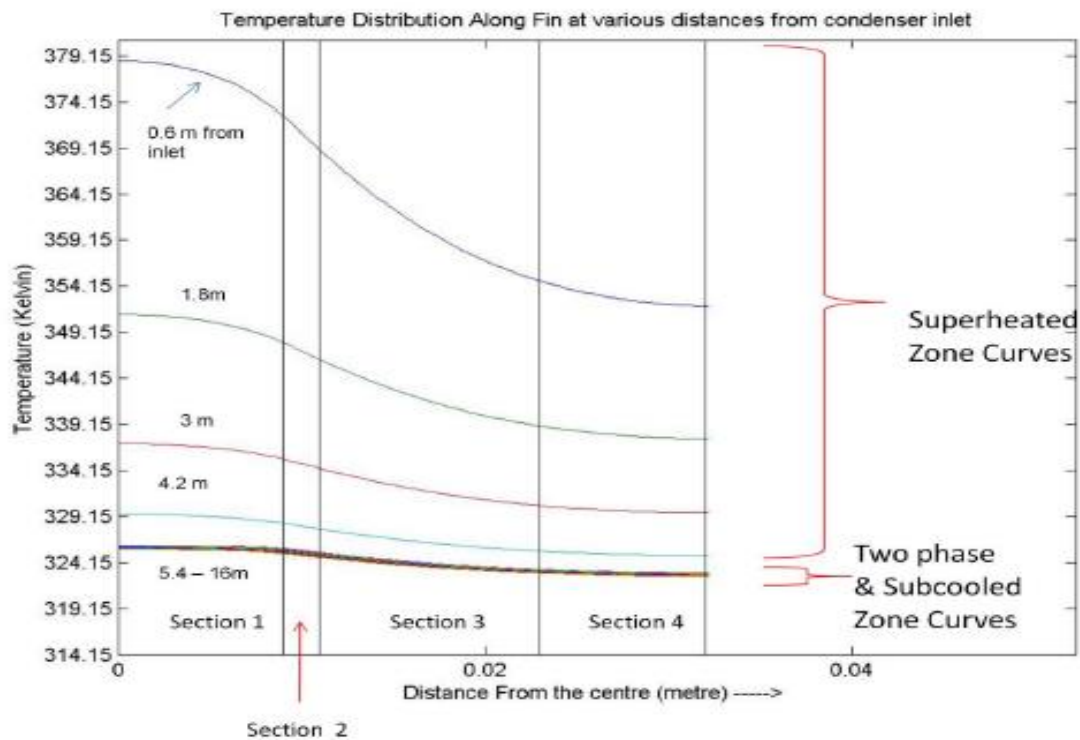


Fig. 8. Temperature Distribution Along Fin at various distances from condenser inlet

3.4 Temperature Distribution Along a cross section of the whole condenser:

Below is the temperature distribution of a cross section of the condenser. Initially when the refrigerant is in the superheated stage the temperature is high. As the refrigerant is cooled in the following tubes it reaches the two phase zone where it temperature remains nearly a constant and thus the distribution looks identical for various tubes in the two phase region.

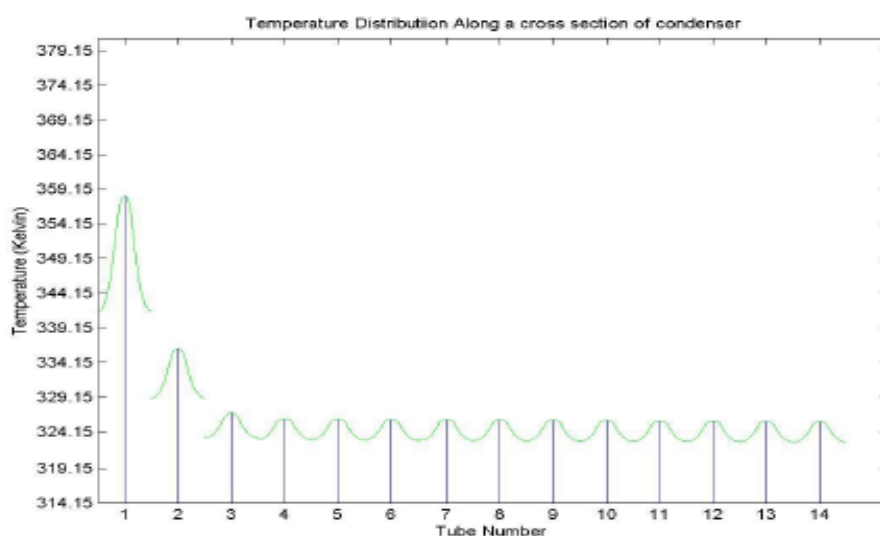


Fig.9 Temperature Distribution along a cross section of condenser.

3.5 Effect of pitch length on results

Parameters	Units	Values			Std. Deviation
Pitch	mm	40	46	50	
Mass Flow Rate	grams/s	0.47848	0.47848	0.47848	-
Exit Temperature	Celsius	52.122079	52.03756	51.98232	0.0704
Exit Pressure	psi	201.5474	201.1238	200.8496	0.3516
Exit Enthalpy	KJ/kg	316.900	304.982	298.779	9.2095
Exit Quality		0.2815095	0.20243	0.161425	0.0610
Total Pressure Drop	psi	3.6810	4.1320	4.3788	0.3538

The above table compares the exit conditions when the pitch is changed. As expected it predicts a larger heat transfer when pitch is increased.

REFERENCES

- [1] NIST, Thermodynamic and Transport Properties of Refrigerants and Refrigerant Mixtures—REFPROP, 6th ed., 1998.
- [2] F.P. Incropera, D.P. De Witt, Fundamentals of Heat and Mass Transfer, third ed., John Wiley & Sons, Inc, New York, 1990.
- [3] Design and modelling of hot-wall condensers in domestic refrigerators ,P.K. Bansal *, T.C. Chin
- [4] Modeling of hot-wall condensers for domestic refrigerators J.K. Gupta, M. Ram Gopal
- [5] Breber, G., Plen, J.W., Taborek, J., 1980. Prediction of horizontal tube side condensation of pure components using flow regime criteria. J. Heat Transfer 102, 471-476.
- [6] Baehr, H.D., Stephan, K., 1998. Heat and Mass Transfer. Springer, Berlin.
- [7] Cavallini, A., Zecchin, R., 1971. High velocity condensation of R-11 vapours inside vertical tubes. Heat transfer in refrigeration, International Institute of Refrigeration, pp. 385-396.
- [8] Jaster, H., Kosky, P.G., 1976. Condensation Heat transfer in a mixed flow regime. Int. J. Heat Mass Trans. 19, 95-99.
- [9] R.w. Lockhart, R.C. Martinelli, Proposed correlation data for isothermal two phase, two-component flow in pipes, Chemical Engineering Proceedings 45 (1949) 39-48.
- [10] S. Kakac, H. Liu, Heat Exchangers Selection, Rating, and Thermal Design, CRC Press, New York, 1998.
- [11] Internal Combustion Engines, By R.K. Rajput.
- [12] Performance Of Reciprocating Compressors, NPTEL, <http://nptel.iitm.ac.in/courses/Webcourse->
- [13] Friedel L. Improved friction pressure drop correlations for horizontal and vertical two phase pipe flow. Ispra European Two Phase Flow Group meet, Paper F2 (1979).